



How bottom-up and top-down controls shape dune topographic variability along the U.S. Virginia barrier island coast and the inference of dune dynamical properties

J. Anthony Stallins¹ · Li-Chih Hsu¹ · Julie C. Zinnert² · Joe K. Brown³

Received: 26 November 2018 / Revised: 27 August 2019 / Accepted: 13 April 2020
© Springer Nature B.V. 2020

Abstract

When topography is incorporated into models of barrier dune dynamical states, how it is represented determines the dynamical properties inferred. Bottom-up representations rely on elevation and localized biogeomorphic modification. Top-down representations incorporate constraints imposed by the spatial patterns of topography. These spatial patterns emerge from island morphological context and the extent localized biogeomorphic processes can expand and structure the larger landscape. We compared topographies across 30 sites among seven barrier islands of the Virginia (U.S.A) coast to gauge the importance of elevation, the bottom-up variable often weighted most in dune biogeomorphic models, relative to top-down patch and continuous surface landscape representations of topography. LiDAR-derived digital elevation models of each site were characterized with non-metric multidimensional scaling to assess how these bottom-up and top-down metrics structured dune topographic variability. Multiple response permutation procedures gauged the strength of topographic differences among sites grouped according to island morphology versus groupings defined by clustering of topographic metrics. Elevation was the dominant metric structuring topography for these low relief islands. Spatial structure was weakly developed. Topographic differences were more robust when based on clusters defined largely by elevational properties rather than by island or island morphological type. For the Virginia barrier islands, storm inputs may more directly shape topography and override landscape-extent top-down spatial structure. The dominance of elevation suggests that resistance may be the more relevant dynamical property for this coast. Properties like resilience may be greater on higher islands with longer storm-free intervals in which biogeomorphic elements can configure relief and act as recursive top-down controls.

Keywords Barrier islands · Biogeomorphology · Dune topography · Disturbance · Resistance · Resilience

Introduction

Descriptions of dune topographic pattern are inferences about how a barrier island may respond to and recover from storm

surge and overwash. The propensity of barrier island morphological types to express specific topographic patterns was one of the first approaches for generalizing about how barrier islands respond to these high water events. Island morphology shapes topography because it reflects the relative importance of wave and tidal energy (Hayes 1979; Davis and Hayes 1984). Island orientation, sediment budgets, climate, bathymetry, and antecedent geology were also recognized as important influences on island morphology and dune topography in these earlier studies (Godfrey 1977; Cleary and Hosier 1979; Godfrey et al. 1979; Short and Hesp 1982). The interaction of dune plants with the prevailing patterns of sediment mobility associated with island morphological types was similarly invoked to account for barrier dune topographic patterns and how they respond to and recover from storm events (Godfrey and Godfrey 1976; Godfrey 1976; Zaremba and Leatherman 1986). Later, overwash-reinforcing and overwash-resisting dynamical states were postulated to

Electronic supplementary material The online version of this article (<https://doi.org/10.1007/s11852-020-00747-7>) contains supplementary material, which is available to authorized users.

✉ J. Anthony Stallins
ja.stallins@uky.edu

¹ Department of Geography, University of Kentucky, Lexington, KY, USA

² Department of Biology, Virginia Commonwealth University, Richmond, VA, USA

³ Integrative Life Sciences, Virginia Commonwealth University, Richmond, VA, USA

develop through these top-down island morphological constraints (Stallins 2005). Long, linear mixed-energy wave-dominated micro-tidal barrier island morphologies were associated with reduced topographic roughness and biogeomorphic feedbacks that lower resistance to incursions of overwash. Shorter and wider tidally-dominated barrier island morphologies were associated with increased topographic roughness and biogeomorphic feedbacks that increase resistance to overwash.

However, barrier island morphology has been shown to exhibit more variability than assumed in the wave and tidal energy relationships originally used to classify them (Stutz and Pilkey 2011; Mulhern et al. 2017). Although the division between mixed-energy wave-dominated versus tidally-dominated island morphologies may be correlated with elevations of the barrier surface, wave-dominated islands are not necessarily lower than tidally-dominated islands. Tidally-dominated morphologies can also be low and overwashed. This conveys that making generalizations about how topography relates to trajectories of response and recovery also requires working from the bottom up. Bottom-up approaches for characterizing topography start with elevation and its variability alongshore. Differences in local elevation become differences in local topography and the basis for generalizing how segments of barrier islands respond to high water events. Overwash-reinforcing and overwash-resisting dynamical states have also been explained through this bottom-up perspectives (Durán and Moore 2015).

Over the last half century, coastal scholars have filled in the continuum of bottom-up and top-down factors shaping topography. Both approaches, top-down and bottom-up, capture relevant aspects of topography. Coastal responses to storm surge and overwash reflect a complexity of multiscalar, nested variables (Phillips 2018; Stallins and Corenblit 2018). From a biogeomorphic perspective, the modification of topography through plant functional types differing in how they trap sediment and respond to burial or erosional disturbance can scale up to shape the larger patterns of topography in the landscape (Odum et al. 1987; Feagin et al. 2005; Schwarz et al. 2018). In turn, this upward assembly of pattern is also shaped by the top-down nearshore factors associated with island morphology. The resulting emergent landscape pattern of topography can in turn have a downward influence on the abiotic and biotic processes that shaped them (Stallins and Corenblit 2018). Yet what merits more circumspection is the extent top-down and bottom-up modes of characterizing topography are incorporated into biogeomorphic dynamical state models for barrier island dunes. Top-down and bottom-up controls on topographic pattern can be expected to vary in strength from one stretch of coast to another. To the extent that models favor bottom-up versus top-down

approaches – often a methodological preference related to academic lineage – different dynamical properties (e.g. Phillips and Van Dyke 2016) of the barrier dunes will be identified and emphasized.

Bottom-up models have substantiated how feedbacks among elevation, the timing of overwash disturbance, and dune vegetation establishment and modification of topography can lead overwash-resisting states or overwash-reinforcing states. However, the patterns that elevations take, their geometry or spatial structure, may contribute an additional top-down influence and shape dynamical properties. Top-down factors contribute to the spatial variability of topography and give an island its topographic distinctiveness beyond just elevation alone. However, top-down island morphological approaches for characterizing topography and inferring dune dynamical properties from them may overgeneralize. The bottom-up model commits the ecological fallacy, assuming that a given elevation will have equivalent dynamical properties elsewhere. Top-down models commit the individualistic fallacy of assuming that the larger nearshore context unproblematically extrapolates to smaller stretches of the coast. As models are all approximations of reality, these fallacies of inference are unavoidable. What may be more worthwhile to consider are the implications of what variables are incorporated into existing dune dynamical models. The kinds of topographic variables that are incorporated into these models determines what kinds of dynamics we can expect on coasts and the generalizations we can make between and within islands (Hsu and Stallins 2020).

We examined how top-down and bottom-up descriptors of dune topography vary in their explanatory strength among and within barrier islands of Virginia (U.S.A), a stretch of the U.S. southeastern Atlantic coast that has representatives of mixed-energy wave-dominated and tidally-dominated island morphologies. Two questions motivated these comparisons: 1) In general, how does dune topography track with island morphology and nearshore context? 2) To what extent can topographic differences on the Virginia islands be attributed to elevational properties versus more spatially-explicit summaries of topographic pattern? Comparisons of topography were made using metrics spanning different geometric attributes of dune elevation observations. They included basic elevational properties as well as those that captured the patch and continuous surface configurations of these elevations.

Background

Early field-based descriptive studies of barrier island process and form took a top-down view of topography. They described the propensity for certain dune topographies to dominate on some island morphologies and their nearshore context more than others (Godfrey 1976, 1977; Cleary and Hosier

1979; Godfrey et al. 1979). A low backsloping topography that peaked in elevation on the front line of dunes was associated with mixed-energy wave-dominated barrier island morphologies. On these long and narrow islands, this topography facilitated the back barrier transport of overwash during high water events (Godfrey and Godfrey 1976; Hosier and Cleary 1977). On mixed-energy wave-dominated barrier islands, ridge-and-swale topography, a much broader island width, and the proximity of tidal inlets was associated with reduced overwash exposure following forcing events. Rather than penetrate inland as on wave-dominated islands, overwash would be redirected by ridge-and-swale topography toward tidal inlets. These scholars also recognized how island orientation, local sediment budget, and tropical and extratropical storm impacts contribute to differences in topography among adjacent islands with similar morphologies. They also introduced how vegetation response and recovery could be an important influence on the spatial patterns of topography. Working mainly on wave-dominated barrier islands, these studies set the stage for our understanding today of how feedbacks between the prevailing overwash forcing regime and plant responses to it shape response and recovery.

With the advent of disturbance theory in ecology (Pickett and White 1985), these feedbacks between dune vegetation, overwash, and topography were expressed in more formal ecological terms. Drawing also from the concept of alternative stable states and resilience theory, biogeomorphic models of the interaction of dune vegetation, elevation, and overwash were developed and refined (Stallins 2005; Wolner et al. 2013; Brantley et al. 2014; Durán and Moore 2015). They describe how biogeomorphic interactions can shape topography and contribute to the expression of a high, overwash-resisting state or a lower, overwash-reinforcing state. A third dynamical condition, bistability, in which either state can occur within an overlapping range of intermediate elevations, was also identified. However, resistance was the central one of two interrelated dynamical properties theorized to arise in these states (Stallins and Corenblit 2018). Resistance refers to properties that directly counter expressions of power from externally-forced disturbances like storm surge. Resilience, is a measure of degrees of freedom a system has evolved to absorb or adjust to disturbance before changing dynamical state (Phillips and Van Dyke 2016; Thoms et al. 2018; Fuller et al. 2019). Resilience has an explicit spatial component. It can become encoded in the abiotic and biotic elements of a landscape (Allen et al. 2016; Cumming et al. 2017; Génin et al. 2018). Whereas a single vegetated dune landform can impart resistance, resilience encompasses how its response and recovery is shaped by the configuration of the larger landscape and how history has shaped the assemblage of topography-modifying organisms.

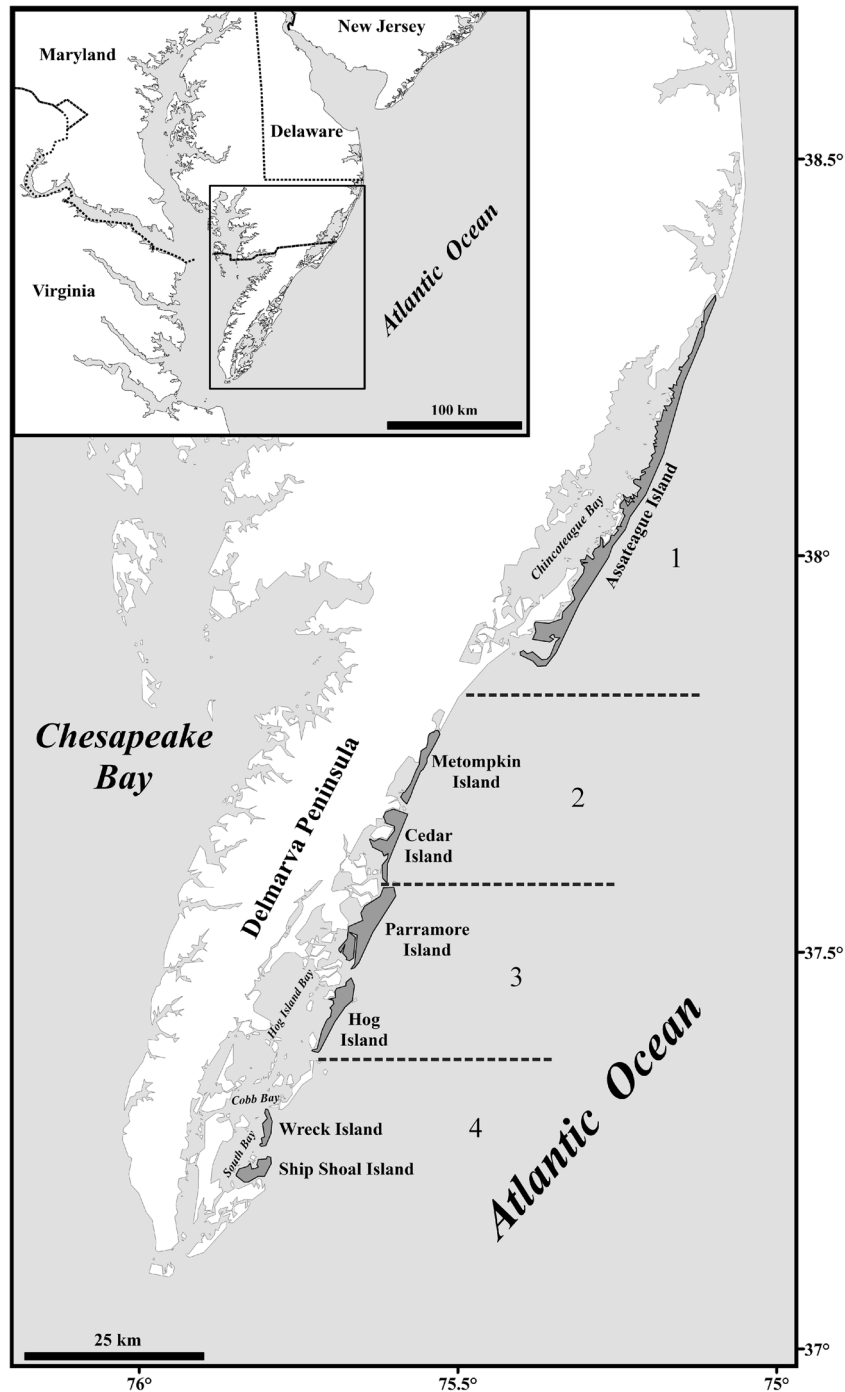
Resistance and resilience reflect an interaction of top-down as well as bottom up factors (Hsu and Stallins 2020). However, many of the spatial, geographically contextual aspects of topography recognized in earlier descriptive studies oriented around island morphology are difficult to incorporate in fine-grained, local-extent bottom-up elevational models. Bottom-up approaches that rely only average elevation, dune crest height, or two-dimensional cross-sectional elevation profiles capture aspects of topography important for understanding their dynamical properties. Yet barrier island dune response and recovery is also a spatial process. By comparing topographies using pattern-process metrics that differ in their degree of spatial explicitness, resolution, and scalar extent, topographic variability not accounted for in the current bottom-up models can become more visible, along with how it is related to resistance and resilience.

Houser et al. (2018) used power laws to document this cross-scale component of barrier island dune response and recovery. The complementary approach employed in our study is to deploy multivariate representations of topography. We compared the dune topographies among seven barrier islands of the Virginia coast using a suite of eighteen topographic metrics. These metrics spanned bottom-up elevational controls to more top-down influences related to the geometry and size of the dune habitat. At an extreme, one can consider that a wide range of dune topographies and dynamical states develop on any single barrier island. The bottom-up variable of elevation varies continuously across the entire barrier surface. Where a barrier island beach reaches its inevitable terminus near a tidal inlet, low flat topography and overwash will inevitably develop, albeit locally, even when higher dunes may characterize extensive stretches of the island. However, assuming that each island contains all possible dune topographies is as unproductive as assuming a specific type of topography will always develop on a particular barrier island morphology. What is more relevant to characterize is the mosaic structure of topography, the predominant assemblages of landforms that develop alongshore (Lane et al. 2017). This is also the basis of the river reach concept, a sampling unit recognizing the distinctive assemblages of landforms that develop in and alongside a river via both top-down and bottom-up controls (Wohl 2018).

Study area

Seven largely undeveloped mixed-energy Virginia barrier islands were selected to make topographic comparisons (Fig. 1; Online Resource 1). The Virginia coast is well-studied, with ample information about shoreline trends and the nearshore conditions that shape island morphology. These islands were also used to validate the predominantly bottom-up model of dune biogeomorphic dynamics (Durán and

Fig. 1 Study area with its four island morphological compartments. Net longshore transport of sediment is to the south



Moore 2015). Rates of relative sea level rise along this coast are among the highest on the US Atlantic coast (Sallenger et al. 2012). Landward retreat rates vary depending upon the time frame examined (Leatherman 1982; Haluska 2017; Deaton et al. 2017). Long-term trends (1851 to 2010) are approximately 1–6 m/year. Short-term retreat rates (1980–2010) for the entire coast are approximately 7 m/year. Virginia barrier islands differ in their shape, size, and sediment

processes, but are responding to sea level rise through parallel and non-parallel retreat (Lorenzo-Trueba and Ashton 2014).

Islands of this stretch of coast have been classified into four coastal compartments based on the geomorphic influences shaping island morphology (Fig. 1; Oertel and Kraft 1994). Wave energy dominates in the most northern compartment. Tidal energy increases in importance to the south. These more southerly tidally-influenced island morphologies have been

segmented into three compartments based on whether islands exhibit parallel or non-parallel retreat, although the type of retreat has been variable over time on some islands (Deaton et al. 2017; Haluska 2017). The northernmost island, Assateague (Table 1), exhibits the long, linear barrier island morphology characteristic of mixed-energy, wave-dominated coasts. Assateague is undergoing parallel retreat (Haluska 2017). It is prone to breaching with numerous ephemeral and long-lived tidal inlets that have formed during extratropical and tropical storms (Seminack and McBride 2015). Anthropogenic modifications of the inlet above Assateague and on Wallops island just below it include sediment dredging. Consequently, downdrift locations on Assateague and islands immediately south experience greater erosion and higher retreat rates (Roman and Nordstrom 1988; Psuty and Silviera 2011).

South of Assateague are the increasingly tidally-influenced barriers of Metompkin Island and Cedar Island. These islands have simple topographies and low elevations that result in frequent overwash during even small extratropical and tropical storms (Brantley et al. 2014). Their coastlines exhibit significant sediment starvation and erosion due to human alteration of sediment budgets on Wallops and Assateague islands. Metompkin is undergoing pervasive rapid retreat. The northern half of Metompkin is retreating faster than the southern half, causing a counter-clockwise rotation (Haluska 2017). Because of rapid retreat, Cedar Island is decreasing in overall area and losing vegetation cover at the expense of bare sand (Nebel et al. 2012; Zinnert et al. 2016).

Parramore Island and Hog Island comprise the next morphological compartment to the south. These islands have relatively high relief (>6 m) and exhibit the distinctive drumstick shape when tidal energy dominates over wave inputs. On Parramore extensive erosion is associated with scarping as the island migrates rapidly landward. The north-central stretch of Parramore is characterized by the truncation of high-profile, tree-lined beach ridges as the island retreats and rolls over into upland forest. Parramore Island's previous clockwise rotational pattern documented by Leatherman (1982) has evolved into a sustained rapid parallel retreat (Haluska 2017). Hog Island also exhibits mostly parallel retreat. However, shoreline retreat rates are lower. Accretion and dune ridge-swale landforms dominate on the northern half of the island, while erosion dominates on the southern half. Hog and Parramore exhibit 'pimple' topography in which erosion during high water events leaves behind circular topographic highs (Hayden et al. 1995). Hog Island differs from the other islands in that it has increased in woody vegetation over the last 40 years (Zinnert et al. 2016).

The most southern compartment of the mixed-energy tide-dominated barrier islands of Virginia consists of Ship Shoal Island and Wreck Island. The diminishment of wave energy is evident in sands that are finer than those to the north (Fenster et al. 2016). Both islands are exhibiting non-parallel shore retreat. Ship Shoal and Wreck also have greater alongshore variability in shoreline changes than the larger islands to the north (Fenster et al. 2016; Haluska 2017). Wreck is retreating faster on its northern part, with the southern end exhibiting shoreline advance seaward. Both islands have had the greatest

Table 1 Island morphologies from north to south. See Fig. 1 for locations

Island	Length (km) ^a	Width (km) ^b	Area (km ²) ^c	Retreat rate (m/yr) ^d
Compartment 1				
Assateague	60.0	0.8	49.2	1.9 ± 0.6
Compartment 2				
Metompkin	10.4	0.3	2.7	10.9 ± 1.0
Cedar	9.6	0.4	4.2	10.8 ± 0.5
Compartment 3				
Parramore	12.8	0.8	9.6	12.4 ± 0.3
Hog	11.2	0.9	9.7	-1.3 ± 0.3
Compartment 4				
Wreck	4.8	0.4	2.1	4.2 ± 1.0
Ship Shoal	2.4	0.4	0.9	6.0 ± 4.8

^a Fenster et al. (2016)

^b Width is summarized as area/length

^c Reported by Zinnert et al. (2016) except for Assateague, Metompkin and Ship Shoal, which were estimated from digitization of aerial photos in Google Earth

^d The retreat rate of Assateague island (2005–2010) is from Psuty and Silveira (2011), other islands are from Deaton et al. (2017) for 1980–2010. Positive values indicate retreat (westward shoreline movement). Negative values indicate advance (eastward shoreline movement)

maximum shoreline retreat of all the Virginia barrier islands (Haluska 2017).

A classification of island morphologies for the U.S. south Atlantic barrier coast by Williams and Leatherman (1993) used island orientation, shoreface concavity, island length and width, wave and tidal measurements, and hurricane exposure to quantitatively cluster barrier island morphologies into distinctive types. Their findings approximated this four morphological compartment model. Assateague Island belonged to a wave-dominated class. Parramore Island was assigned to the widest-island class. Metompkin, Cedar, and Hog islands were allocated to an outlier class, which Kochel et al. (1983, p. 50) described as islands lacking “geomorphic organization.” Wreck and Ship Shoal islands were classified into the shortest-island class, typifying tidally-dominated island morphologies strongly influenced by antecedent topography. Monge (2014) classified this same stretch of U.S. coast using many of the variables employed by Williams and Leatherman (1993). Their results more closely followed the four compartment model in which Assateague Island was classified into its own group, and the remaining six barrier islands formed three morphological groupings comprising Metompkin and Cedar, Hog and Parramore, and Wreck and Ship Shoal. The island morphological controls used in these classifications are top-down variables. However, they are difficult to parameterize for individual sites along an island in order to compare their influence to that of bottom-up elevation. To work around this constraint, spatially-explicit patch and gradient patterns of topography were used to represent these geographically-contingent nearshore influences. These can be more readily quantified and compared to elevation within and among different barrier islands.

Data

Topographically distinctive, contiguous coastal reaches within each of the study islands were visually identified in Google Earth imagery. The time frame was constrained to the most recent years LiDAR data were available that spanned multiple islands. Criteria to detect the predominant topographies defining the landscape mosaic of an island included beach width, the width of the dune field, linearity of the dunes, and type of habitat behind dunes. Areas of pervasive human impact and locations directly on tidal inlets were excluded. Three to five distinctive stretches of topography were adequate to capture the range of topographies on each island (Figs. 1, 2 and 3; Online Resource 1), yielding 30 sites total. Square plots were randomly located within each distinctive stretch of barrier island dune shoreline. They initiated at the mean high water mark datum (MHW) and up through any fronting primary foredunes and across the backshore until the occurrence of salt marsh or significant stabilized woody vegetation. Thus

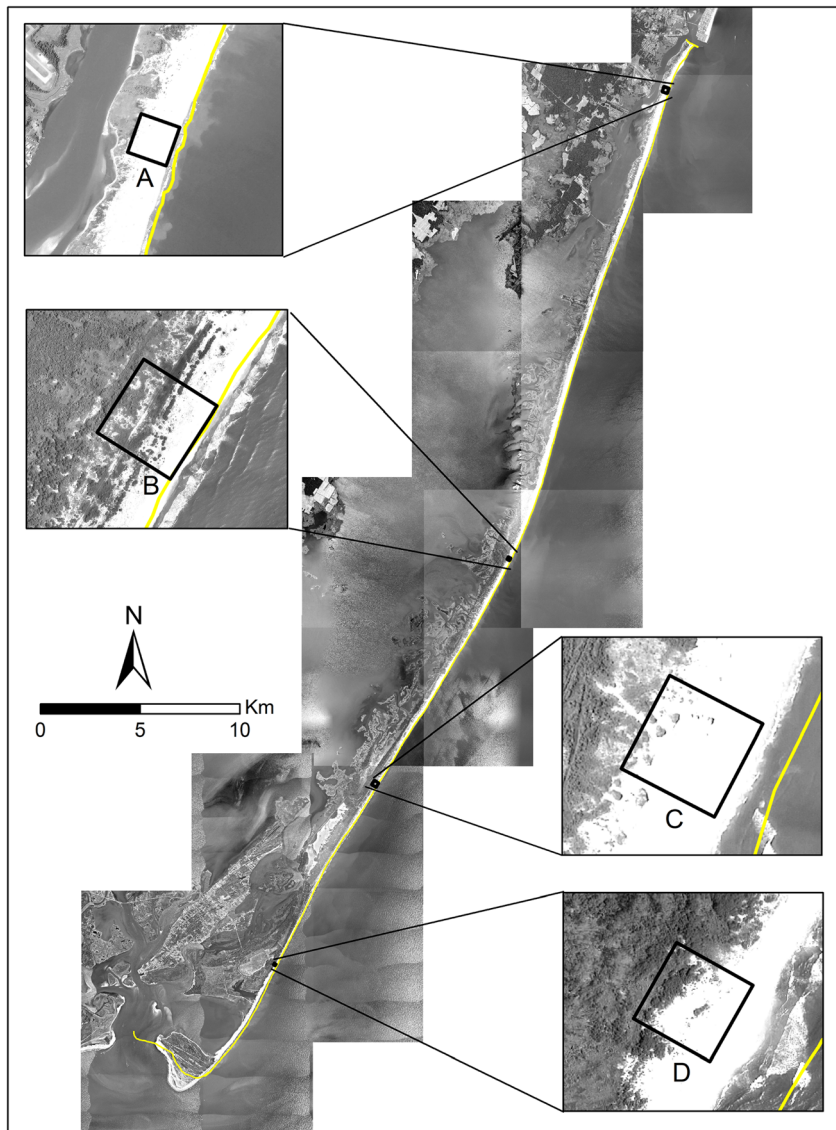
the study sites encompass dune topographic variability within an area rather than focusing on primary foredune height or an average elevation.

Digital elevation models were constructed for each site plot from LiDAR ground elevation data available online from the NOAA’s Coastal Services Center. A post-Sandy 2014 dataset collected by the NOAA National Geodetic Survey was used for all seven islands. Vertical (horizontal) accuracy was 6.2 cm (100 cm) and nominal point space was 0.3 m. In each of the plots, LiDAR point elevations were resampled to a resolution of 1 m and then interpolated using inverse distance weighing to fill any gaps. LiDAR processing was performed in ArcGIS using LAStools. The MHW shoreline was defined as the 0.7 m contour line relative to the NAVD 88 datum (Rogers et al. 2015).

To represent the bottom-up aspects of topography incorporated into the existing models of barrier dune dynamical states, site elevations were summarized in terms of descriptive statistics (mean, 25th, 50th, and 75th percentiles) for the 1-m DEM surface in GS+ software (Robertson 2000). To capture aspects of topography that have an increasing top-down component, DEM elevations were classified into decimeter intervals. This was done in order to quantify the patch structure of elevation (Wu et al. 2017). A patch in this sense is the areal form taken by these decimeter elevation intervals. Details of the patch structure were characterized with FRAGSTATS, a widely used tool for quantifying the attributes of patches that comprise a landscape (McGarigal et al. 2012). Eight indices were selected. The aggregation index (AI) increases with greater patch coalescence and size. The area-weighted mean shape index (SHAPE_AM) increases as patches become more curvilinear. Higher values for the interspersion and juxtaposition index (IJI) indicate that patches are equally adjacent to all other patches. Higher values for the largest patch index (LPI) imply a greater dominance of a single patch type. A higher Simpson’s diversity index (SIDI) implies higher patch richness and more equitable patch abundance. For the perimeter-area fractal dimension index (PAFRAC), all patch shapes tend to be convoluted when this value is large. The contagion index (CONTAG) increases as patches become larger and dominated by a single elevational range.

The third set of metrics characterized the properties of the continuous elevation surface expressed at landscape extents. These more top-down variables reflect more of the contingent spatial pattern taken by dunes in response to nearshore conditions that set the context for island morphology. They included the skewness and kurtosis of point elevation values, plot size, and the autocorrelation structure of elevations. Autocorrelation structure was derived from directional (perpendicular to the water line) correlograms for each DEM plot. Moran’s *I* values from the major breaks along each plot’s directional correlogram were ordinated with principal coordinates analysis (PCoA) in order to distill correlogram structure into coordinates that could then

Fig. 2 Study plots on Assateague Island. Letters indicate position along island, from A (northernmost) to E (southernmost)



ordinated with the other dune topographic metrics. Changes in skewness, kurtosis, and autocorrelation of driving variables have been associated with changes in dynamical states (Scheffer et al. 2015). Because topographic metrics were measured in different units, they were standardized as Z-scores in the final data set (Online Resource 2).

Statistical analyses

Topographic variability among sites and islands was assessed using non-metric multidimensional scaling (NMDS). An orthogonal rotation of the solution maximized topographic variability on the first and then succeeding axes. Pearson's correlation coefficients were calculated for the NMDS scatterplot coordinates and the original topographic metrics. These correlations indicated the relative importance of individual topographic metrics. An ordination with PCoA was also

performed to derive the percent variance extracted along these axes. The topographies for island sites were clustered using a hierarchical agglomerative algorithm and a flexible beta linkage method. Multiresponse permutation procedures (MRPP) were used to test for significant differences in site topography among these clusters, among islands, and among the four island morphological compartments comprising the Virginia coast. All statistical analyses were performed using PC-Ord Version 7 (McCune and Mefford 2016). Similarity distances were Euclidean.

Results

The distribution of point elevations in each site DEM was wider toward Assateague in the north (Fig. 4). Lower and less variable point elevations tended to develop on the

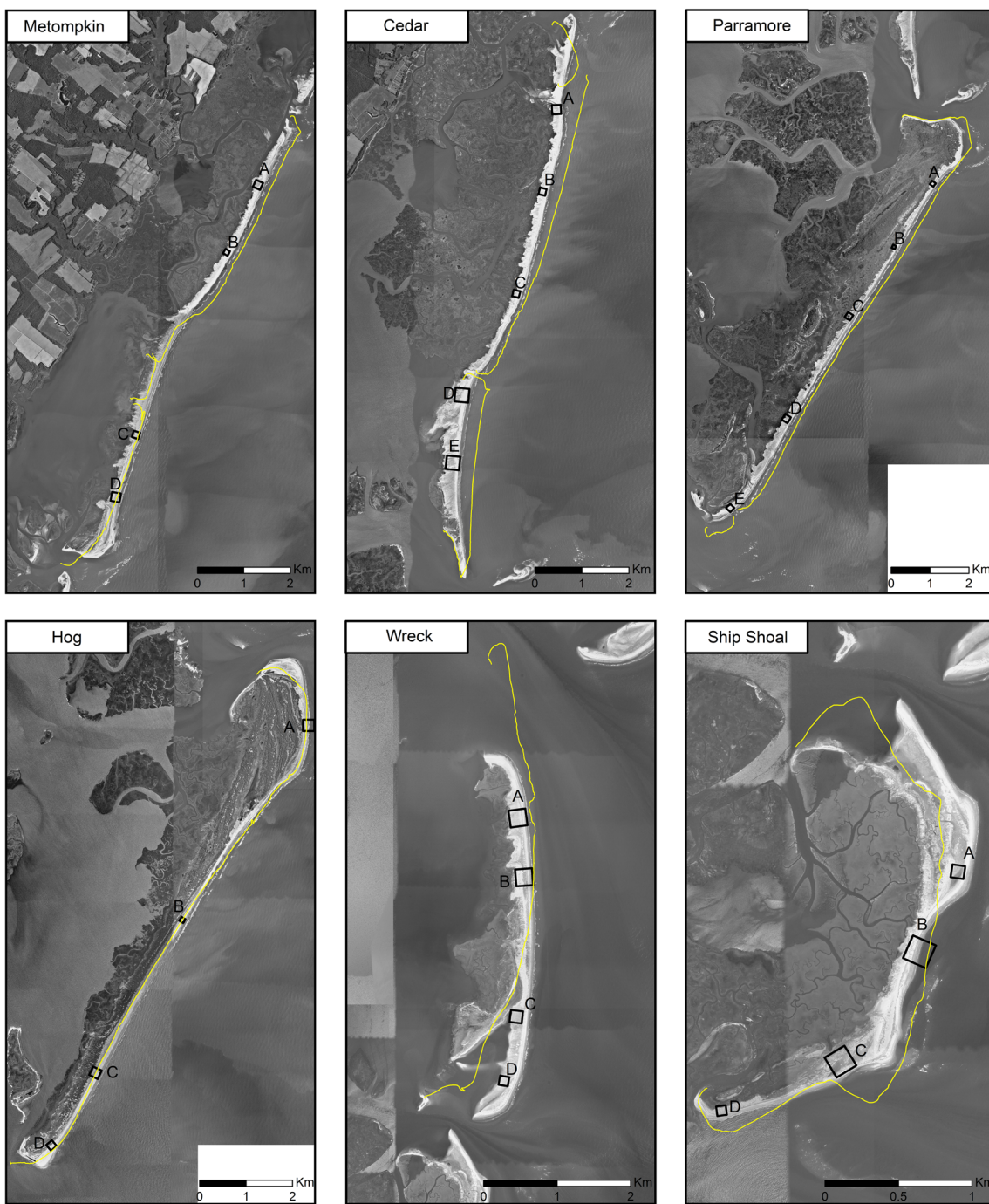


Fig. 3 Study sites. Wave energy decreases as tide energy increases from Metompkin to Ship Shoal. The yellow line is the approximate shoreline in 1994 based on the location of the high water mark for each island derived

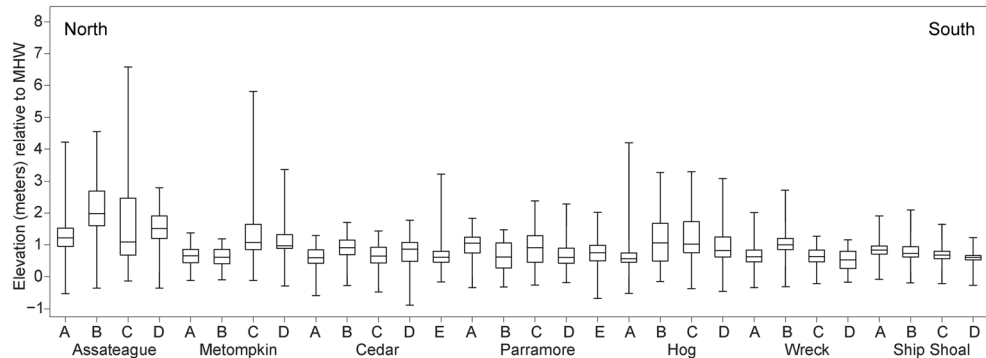
from Google Earth Imagery. Aerial photos are from the National Agriculture Imagery Program (2011)

southernmost barrier islands of Ship Shoal and Wreck. In general, the differences in elevation among islands and island sites may be more strongly related to its variability than central tendency. Mean elevations among all islands were close to 1 m. Despite this similarity in mean site position above the HWM, these elevations formed a range of topographies (Fig. 5), varying from uniform to heterogeneous and patchy (Wreck D vs. Assateague A). Some sites had topographic

highs close to the high water mark while others peaked in elevation toward the rear of the site (Parramore B vs. Metompkin C) possibly due to erosion on the front half. Topography also differed in the predominance of shore-parallel versus cross-shore orientations of dune topography (Wreck D vs. Assateague B).

The patch structure of elevation varied among sites. The aggregation index differentiated large, continuous patches of

Fig. 4 Boxplots of elevation in 1-m cells for each plot. The central mark indicates the median, and the bottom and top edges of the box indicate the 25th and 75th percentiles, respectively. The whiskers extend to the maximum and minimum values



elevation (for example Cedar A, AI = 91.8) from smaller, less aggregated patches (Assateague C, AI = 53.3). SHAPE_AM distinguished between curvilinear patch structure (Cedar D, 5.5) and rectangular patch structure (Hog B, 2.9). IJI identified how elevations varied from clumpy (Ship Shoal C, 47.8) to uniformly dispersed (Hog B, 61.5). Patch diversity (SIDI), the number and equitability of different elevational intervals, ranged from a low on Ship Shoal D (0.77) to a high on Assateague B (0.96). The extent a single large patch of elevation (LPI) dominated a site ranged from a low on Assateague C (2.4) to a high on Ship Shoal D (36.2).

A two-dimensional NMDS solution was optimal for the topographic metrics (Fig. 6). Stress reduction for this solution was significantly greater than solutions derived from ordinations of Monte Carlo randomizations of the data ($p = 0.004$ for both axes, $n = 249$). Final mean stress was 11.5. PCoA indicated that the first axis extracted 43.7% of the variance. The second axis contributed approximately a third, or 22.2%, of the total variance in the data set (65.9%). Assateague's wave-dominated topography was distinctive from the other islands. The other more tidally-dominated islands had overlapping topographies. Neither islands nor morphological compartments were topographically distinctive. Tidally-dominated islands covered a large area of the total topographic state space despite sizes smaller than Assateague.

Bottom-up properties had a dominant influence of the dune topographic structure of the Virginia barrier islands. Based on Pearson's correlations with the first axis (Table 2), elevational descriptive statistics had the strongest influence on topography, excepting maximum elevation. Despite the importance of elevation, site DEMs had little consistent variability in spatial structure. Only the aggregation index (AI) and patch diversity (SIDI) also had strong correlations with the first axis. Plot size, and the skewness and kurtosis of elevations had strong correlations with the second NMDS axis.

The tendency for cluster groups to be comprised of sites solely from the same island or exclusively from any one of the four morphological compartments was weak (Fig. 7). Affinities to cluster with a neighboring within island site or an adjacent island were also not an overriding influence. At

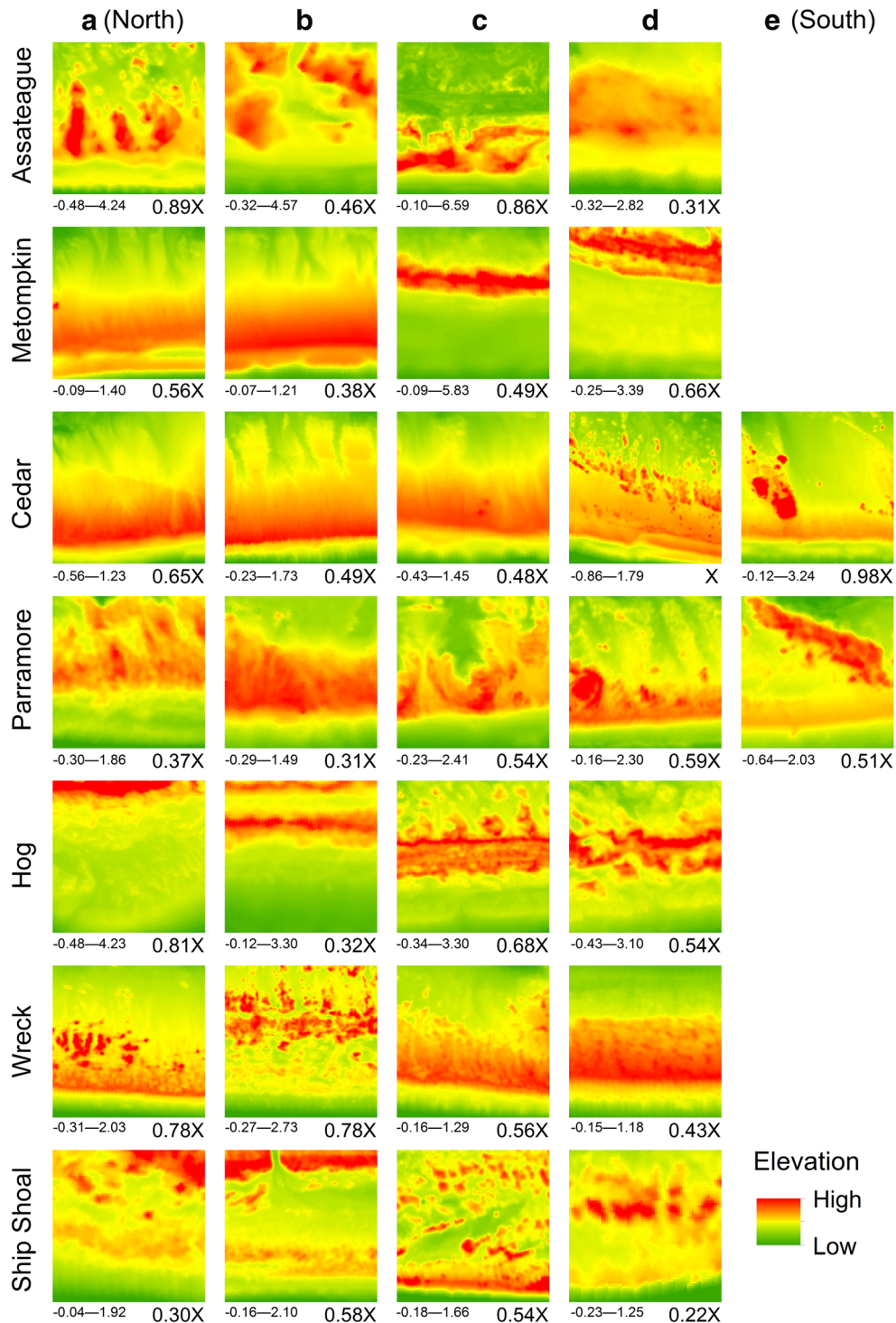
the level of two clusters, Assateague combined with plots from Hog and Parramore instead of with those on Metompkin and Cedar, closer islands just south below it. The other cluster comprised the plots of the rapidly retreating, rotating islands of Metompkin and Cedar as well as the low relief plots on Wreck and Ship Shoal. At four clusters, topography organized into a northern high wave energy cluster dominated by Assateague, a less erosional cluster of plots from Hog and Parramore, and a third cluster of very low elevation plots chiefly from Wreck and Cedar. Top-down spatial properties (skewness, kurtosis, and plot size) differentiated sites along the second axis only at the level of seven clusters (Fig. 8).

MRPP detected significant differences in topography when grouped by island, by the four morphological compartments and for cluster groupings (Table 3). However, the robustness of this significance varied. The A values were highest for the three- and four-cluster groupings, an indication of the robustness of these groupings of topographic similarity over those based solely on island or island morphology. A values closer to zero indicate a difference no greater than expected by chance.

Discussion

Wave-dominated barrier islands have been assumed to be low, overwash-reinforcing islands. Tide-dominated islands have been assumed to be high, overwash-resisting islands. However, in this study, the opposite situation existed. The lower and more reduced topographies were expressed on tide-dominated barrier island morphologies. The dune topographies of the Virginia barrier islands formed three groups structured along a gradient of elevation that approximated but were not exclusive to island morphological compartments: 1) a cluster of higher, positive dune relief on wave-dominated Assateague Island; 2) a cluster of more erosional remnant dune relief dominated by Hog and Parramore islands, and 3) a cluster of very low, flat, topography on Cedar, Metompkin, Ship Shoal, and Wreck. This conveys how within-island elevational variability may

Fig. 5 Site DEMs. The HWM is approximate to the lower edge of each site DEM. Letters indicate position along island, from A (northernmost) to E (southernmost). Sites differed in size although shown the same here. Conversion factors below each raster can be used to derive their size relative to the largest island plot, Cedar D (295×295 m). For example, the actual dimensions of Assateague plot A are 262×262 m ($0.89 \times 295 = 262$ m)



override the potential for island morphological identity to constrain topography. As one example, although geographically closer to Assateague Island, some of the plots on Metompkin and Cedar were more similar to those of Wreck and Ship Shoal, the southernmost islands of the study area. Coastline engineering on Assateague and Wallops Island to the south of it are likely responsible for

downdrift sediment starvation and the enhanced erosion and retreat on Metompkin and Cedar.

To further detail the extent within-island topography could override island morphology, we paired the coordinates of sites in our investigation with Haluska's (2017) reconstruction of alongshore trends in erosion and accretion for the Virginia barrier islands (Table 4). Based on Haluska's data, the

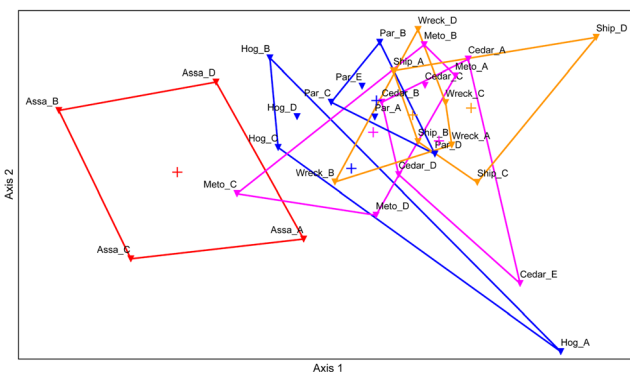


Fig. 6 NMDS scatterplot of site topographies grouped by island and color coded according to island morphological compartment shown in Fig. 1

locations of the A and B plots on Metompkin were highly erosional while the locations for the C and D plots were much less so. In the NMDS scatterplot, dune topographies for Metompkin C and D plots were grouped into the cluster group consisting of the less erosional topographies on Hog and Parramore islands. Metompkin A and B plots were clustered with the low relief erosional plots on Ship Shoal and Wreck, as would also be expected based on Haluska's measurements. Thus, island morphology on low erosional coasts may set the

Table 2 Pearson's correlation coefficients for plot NMDS axis coordinates and topographic metrics for Virginia barrier islands. Stronger correlations designated as those equal to or exceeding ± 0.70

	Axis 1	Axis 2
Elevational descriptive statistics		
Mean elevation	-0.91	-0.24
Max elevation	-0.64	-0.65
25th percentile elevation	-0.70	-0.17
50th percentile elevation	-0.85	-0.08
75 percentile elevation	-0.95	-0.14
Patch metrics		
Aggregation index	0.80	0.15
Contagion	0.64	-0.65
Interjuxtaposition	-0.66	0.33
Large patch index	0.63	-0.02
Landscape shape index	-0.60	-0.59
Perimeter-area fractal dimension	-0.62	-0.15
Mean shape index	0.65	-0.44
Patch diversity	-0.81	-0.04
Continuous surface metrics		
Skewness of point elevations	0.04	-0.77
Kurtosis of point elevations	0.39	-0.74
Directional spatial autocorrelation of elevation	0.14	-0.38
Plot size	0.06	-0.78

Bold numbers are significant ($p < 0.01$)

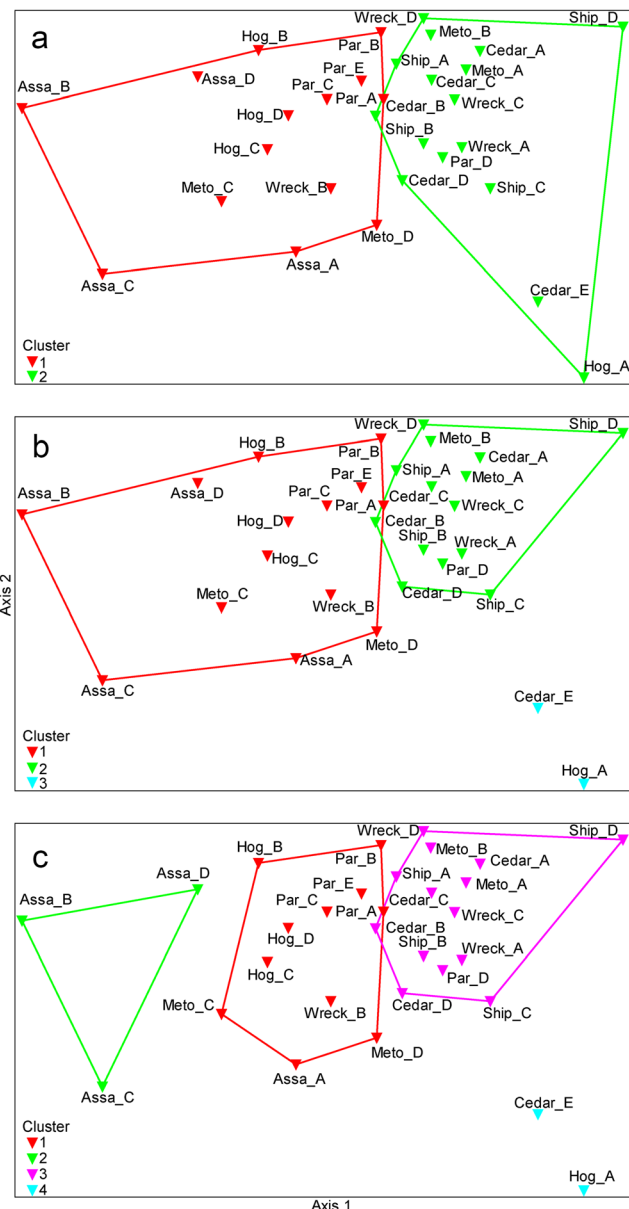


Fig. 7 NMDS scatterplots of dune topography for 2, 3 and 4 cluster group solutions

stage for the expression of a particular dune topography, but local patterns of erosion and accretion may override it. Island morphology and spatial patterning is not as useful a tool to discriminate dunes of the Virginia barrier islands as is elevation.

Based on the position of island sites in the NMDS scatterplot, topographic contrasts were nearly as large on morphologies where tidal energy dominates over wave energy. Even with their much smaller island dimensions, topographies on the smaller tidally-dominated islands of Virginia were as wide-ranging as those on the more wave-dominated island of Assateague. This may be because tide-dominated barriers in general exhibit a range of retreat behaviors more frequently than wave-dominated barrier islands. The greater adjacency of

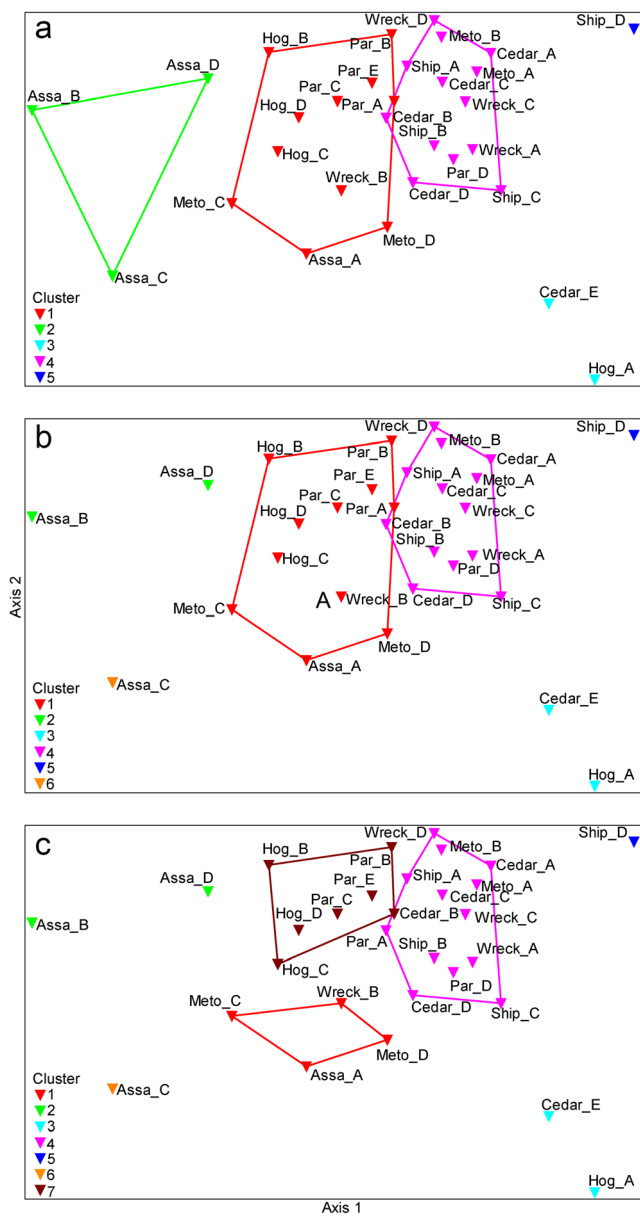


Fig. 8 NMDS scatterplots of dune topography for 5, 6 and 7 cluster group solutions

tidal inlets that serve as sources and sinks for sediment and the switching between parallel to rotational retreat likely enhance the topographic variability among sites of tidally-

Table 3 MRPP results. All significant $p < 0.001$

Grouping	T	A
2 Clusters	-10.88	0.12
3 Clusters	-10.09	0.19
4 Clusters	-10.08	0.23
Morphological compartment	-5.67	0.12
Island	-4.58	0.14

Table 4 Annual shoreline movement rate for each island (1990–2014) inferred from graphical results presented in Haluska (2017). Distance is the location alongshore in km starting from the southern terminus of each island

Island	Plot	Distance (km)	Shoreline movement rate(m/year)
Metompkin	A	8.70	-10.00
	B	7.26	-13.00
	C	2.86	-1.00
	D	1.43	2.00
	E		
Cedar	A	10.64	-22.00
	B	8.65	-15.00
	C	6.43	-10.00
	D	3.86	-15.00
	E	2.34	-18.00
Parramore	A	11.11	-10.00
	B	9.46	-12.00
	C	7.04	-10.00
	D	3.74	-15.00
	E	0.99	-20.00
Hog	A	11.15	7.00
	B	6.79	-1.00
	C	2.71	2.00
	D	0.68	5.00
Wreck	A	3.94	-10.00
	B	3.36	-5.00
	C	0.87	28.00
	D	0.29	45.00
Ship Shoal	A	2.03	8.00
	B	1.45	-2.50
	C	0.58	-6.00
	D	0.08	-8.00

dominated islands in Virginia. Based on Phillips (1999), geomorphic processes can diversify topography over short distances, as observed for the smaller tidally-dominant islands in this study. However, although within-island topography on them was divergent, the islands collectively occupied an overlapping region in the NMDS topographic state space. This suggests the potential for the homogenization of relief analogous to the increasing homogenization in dune cover over time observed by Zinnert et al. (2019). For the higher, more wave-dominated island of Assateague, a similar range of topographic variability was expressed, but it developed over a much larger island size. This suggests a convergence instead of a divergence in topography. Assateague still retains a more consistent overwash topography in which elevation peaks along the fronting dune line and becomes gradually lower in backshore direction.

On the Virginia barrier islands, bottom-up elevational properties dominated over top-down controls. This is not

surprising as elevation relative to a datum is an important factor in many coastal habitats. However, the lack of any strong, consistent spatial structure to these elevations suggests that frequent storm inputs may be the more direct and pervasive influence on dune topography for the Virginia coast. Elevation, as represented in terms of its patch structure, had little systematic variability with the exception of the aggregation index and patch diversity. Elevational skewness, kurtosis, and the area over which these elevations were expressed also had an explanatory component. But these metrics differentiated only a few non-outlier sites from others (Fig. 8c), indicating their weak influence on overall topographic variability.

The lack of organized spatial structure suggests that top-down controls imposed through biogeomorphic processes operative at extents greater than individual plant populations and localized dune landforms are weakly expressed for the Virginia coast. When return intervals for overwash-forcing events are small, there may not be enough time for small hummocky dunes to coalesce into larger continuous landscape features that would constrain spatial structure by modulating overwash exposures (Goldstein et al. 2017). Consequently, elevation in the context of the Virginia barrier islands may reflect resistance to storm inputs more than resilience. Applying bottom-up models in areas that are higher and less frequently overwashed may capture resistance, but the biogeomorphic resilience encoded in the spatial structure of dunes and vegetation may go undetected. Insofar as the Virginia barrier islands are resilient, it is in the capacity that resistance has some collinearity with resilience. Vegetation recovery and the direct anchoring effects of vegetation are the likely contributors to this resilience more than spatial configuration of dune landforms and plant functional abundances. Biogeomorphic studies in a variety of coastal habitats have documented that the spatial pattern of interacting geomorphic and biotic elements contributes to resilience (Rietkerk and van de Koppel 2008; Weerman et al. 2010; Yousefi Lalimi et al. 2017; Schwarz et al. 2018). As this spatial and biotic aspect of dune landform resilience diminishes, it may enhance the potential for more rapid erosion and retreat in association with inlet dynamics (Fitzgerald et al. 2018).

Conclusion

For the Virginia barrier coast, island morphology shaped topography but mainly for the division between wave- and tidally-dominated barrier islands. In the tidally-dominated island morphological compartments, local shoreline trends in accretion and erosion were responsible for much of the variability in topography. Elevation above a tidal datum appears to be an overriding influence on topography across all scalar extents. Consequently, topography may reflect the direct imprint of meteorological forcings more than it does any

landscape-extent structure emerging from biogeomorphic feedbacks. The dominance of these absolute measures of elevation suggests that for this coast, resistance may be the overriding dynamical property. The potential for resilience may be greater on coasts that are higher and have longer storm-free intervals in which biogeomorphic elements can configure relief at broader spatial extents and act as recursive top-down controls. The findings of this study are applicable to other barrier systems. They convey that a larger accounting for topographic variability is a necessary step to understanding the range of dynamical properties that can emerge along barrier coasts. Comparing dune topographic patterns in Virginia with those from across the Georgia Bight or along the barrier islands of northern Europe could provide a better picture of dune topographic state space and the dynamical properties expressed within it. Nonetheless, it is likely that coastal planners, modelers, and ecologists will differ in the importance they attach to accounting for the multiple attributes of topographic pattern and the kinds of dynamical properties that can be inferred from them. Resistance as a function of elevation may be the more strategic property to prioritize under the presently unfolding scenario of rapid sea level rise. For coastal conservation, the conditions under which high resilience may develop may already be diminished and infrequently encountered.

References

- Allen CR, Angeler DG, Cumming GS, Folke C, Twidwell D, Uden DR, Bennett J (2016) Quantifying spatial resilience. *J Appl Ecol* 53(3): 625–635. <https://doi.org/10.1111/1365-2664.12634>
- Brantley ST, Bissett SN, Young DR, Wolner CW, Moore LJ (2014) Barrier island morphology and sediment characteristics affect the recovery of dune building grasses following storm-induced overwash. *PLoS One* 9(8):e104747. <https://doi.org/10.1371/journal.pone.0104747>
- Cleary W, Hosier P (1979) Geomorphology, washover history, and inlet zonation: Cape Lookout, NC to Bird Island, NC. In: Leatherman SP (ed) *Barrier Islands: From the Gulf of St. Lawrence to the Gulf of Mexico*. Academic, New York, pp 237–271
- Cumming GS, Morrison TH, Hughes TP (2017) New directions for understanding the spatial resilience of social–ecological systems. *Ecosystems* 20(4):649–664. <https://doi.org/10.1007/s10021-016-0089-5>
- Davis RA, Hayes MO (1984) What is a wave-dominated coast? *Mar Geol* 60(1–4):313–329. [https://doi.org/10.1016/0025-3227\(84\)90155-5](https://doi.org/10.1016/0025-3227(84)90155-5)
- Deaton CD, Hein CJ, Kirwan ML (2017) Barrier island migration dominates ecogeomorphic feedbacks and drives salt marsh loss along the Virginia Atlantic Coast, USA. *Geology* 45(2):123–126. <https://doi.org/10.1130/G38459.1>
- Durán O, Moore LJ (2015) Barrier island bistability induced by biophysical interactions. *Nat Clim Chang* 5(2):158–162. <https://doi.org/10.1038/nclimate2474>
- Feagin RA, Wu XB, Smeins FE, Whisenant SG, Grant WE (2005) Individual versus community level processes and pattern formation

- in a model of sand dune plant succession. *Ecol Model* 183(4):435–449. <https://doi.org/10.1016/j.ecolmodel.2004.09.002>
- Fenster MS, Dolan R, Smith JJ (2016) Grain-size distributions and coastal morphodynamics along the southern Maryland and Virginia barrier islands. *Sedimentology* 63(4):809–823. <https://doi.org/10.1111/sed.12239>
- FitzGerald DM, Hein CJ, Hughes Z, Kulp M, Georgiou I, Miner M (2018) Runaway barrier island transgression concept: Global case studies. In: Moore L, Murray AB (eds) *Barrier dynamics and response to changing climate*. Springer, Cham, pp 3–56
- Fuller IC, Gilvear DJ, Thoms MC, Death RG (2019) Framing resilience for river geomorphology: reinventing the wheel? *River Res Appl* 35(2):91–106. <https://doi.org/10.1002/rra.3384>
- Génin A, Majumder S, Sankaran S, Schneider FS, Danet A, Berdugo M, Gutta V, Kéfi S (2018) Spatially heterogeneous stressors can alter the performance of indicators of regime shifts. *Ecol Indic* 94(1): 520–533. <https://doi.org/10.1016/j.ecolind.2017.10.071>
- Godfrey PJ (1976) Comparative ecology of east coast barrier islands: hydrology, soil, vegetation. In: Barrier islands and beaches: Technical Proceedings of the 1976 Barrier Island workshop. The Conservation Foundation, Annapolis, pp 5–34
- Godfrey P (1977) Climate, plant response and development of dunes on barrier beaches along the US east coast. *Int J Biometeorol* 21(3): 203–216. <https://doi.org/10.1007/BF01552874>
- Godfrey PJ, Godfrey MM (1976) Barrier island ecology of Cape Lookout National Seashore and vicinity, North Carolina. U.S. Government Printing Office, Washington, DC
- Godfrey P, Leatherman S, Zaremba R (1979) A geobotanical approach to classification of barrier beach systems. In: Leatherman SP (ed) *Barrier islands: From the Gulf of St. Lawrence to the Gulf of Mexico*. Academic, New York, pp 99–126
- Goldstein EB, Moore LJ, Durán-Vincent O (2017) Lateral vegetation growth rates exert control on coastal foredune hummockiness and coalescing time. *Earth Surf Dyn* 5(3):417–427. <https://doi.org/10.5194/esurf-5-417-2017>
- Haluska JD (2017) Analysis of Virginia Barrier Island shoreline movement and correlations to sea level and wave height changes and teleconnection patterns. Dissertation, Old Dominion University
- Hayden BP, Santos MCFV, Shao G, Kochel RC (1995) Geomorphological controls on coastal vegetation at the Virginia coast reserve. *Geomorphology* 13(1):283–300
- Hayes M (1979) Barrier island morphology as a function of tidal and wave regime. In: Leatherman SP (ed) *Barrier Islands from the Gulf of Mexico to the Gulf of St. Lawrence*. Academic, New York, pp 1–28
- Hosier PE, Cleary WJ (1977) Cyclic geomorphic patterns of washover on a barrier island in southeastern North Carolina. *Environ Geol* 2(1): 23–31. <https://doi.org/10.1007/BF02430662>
- Houser C, Wernette P, Weymer BA (2018) Scale-dependent behavior of the foredune: implications for barrier island response to storms and sea-level rise. *Geomorphology* 303:362–374. <https://doi.org/10.1016/j.geomorph.2017.12.011>
- Hsu LC, Stallins JA (2020) Multiple representations of topographic pattern and geographic context determine barrier dune resistance, resilience, and the overlap of coastal biogeomorphic models. *Ann Assoc Am Geogr* 110(3):640–660
- Kochel RC, Kahn JH, Dolan R, Hayden BP, May PF (1983) Mid-Atlantic barrier coast classification. Technical report 27, Office of Naval Research, Arlington, VA. Retrieved 5 July 2019 from <https://apps.dtic.mil/docs/citations/ADA128994>
- Lane BA, Pasternack GB, Dahlke HE, Sandoval-Solis S (2017) The role of topographic variability in river channel classification. *Prog Phys Geogr* 41(5):570–600
- Leatherman SP (1982) Barrier island handbook. Coastal Publications, Charlotte
- Lorenzo-Trueba J, Ashton AD (2014) Rollover, drowning, and discontinuous retreat: distinct modes of barrier response to sea-level rise arising from a simple morphodynamic model. *Journal of Geophysical Research: Earth Surface* 119(4):779–801. <https://doi.org/10.1177/0309133317718133>
- McCune B, Mefford MJ (2016) PC-ORD. Multivariate analysis of ecological data. Version 7. MjM software design, Gleneden Beach, OR
- McGarigal K, Cushman SA, Ene E (2012) FRAGSTATS v4: spatial pattern analysis program for categorical and continuous maps. University of Massachusetts at Amherst, MA. Retrieved July 5, 2019 from <http://www.umass.edu/landeco/research/fragstats/fragstats.html>
- Monge JA (2014) Convergence of dune topography among multiple barrier island morphologies. Master Thesis, University of Kentucky
- Mulhern JS, Johnson CL, Martin JM (2017) Is barrier island morphology a function of tidal and wave regime? *Mar Geol* 387:74–84. <https://doi.org/10.1016/j.margeo.2017.02.016>
- Nebel SH, Trembanis AC, Barber DC (2012) Shoreline analysis and barrier island dynamics: decadal scale patterns from Cedar Island, Virginia. *J Coast Res* 28(2):332–341. <https://doi.org/10.2112/JCOASTRES-D-10-00144.1>
- Odum WE, Smith TJ, Dolan R (1987) Suppression of natural disturbance: long-term ecological change on the outer banks of North Carolina. In: Turner MG (ed) *Landscape heterogeneity and disturbance*. Springer, New York, pp 123–135
- Oertel G, Kraft J (1994) New Jersey and Delmarva barrier islands. In: Davis RA (ed) *Geology of Holocene Barrier Island Systems*. Springer-Verlag, Berlin Heidelberg, pp 207–232
- Phillips JD (1999) Divergence, convergence, and self-organization in landscapes. *Ann Assoc Am Geogr* 89(3):466–488. <https://doi.org/10.1111/0004-5608.00158>
- Phillips JD (2018) Coastal wetlands, sea level, and the dimensions of geomorphic resilience. *Geomorphology* 305:173–184. <https://doi.org/10.1016/j.geomorph.2017.03.022>
- Phillips JD, Van Dyke C (2016) Principles of geomorphic disturbance and recovery in response to storms. *Earth Surf Proc Land* 41(7): 971–979. <https://doi.org/10.1002/esp.3912>
- Pickett STA, White PS (1985) The ecology of natural disturbance and patch dynamics. Academic Press, San Diego
- Psuty N, Silveira T (2011) Monitoring shoreline change along Assateague barrier island: the first trend report. *J Coast Res SI* 64: 800–804 (Proceedings of the 11th International Coastal Symposium)
- Rietkerk M, van de Koppel J (2008) Regular pattern formation in real ecosystems. *Trends Ecol Evol* 23(3):169–175. <https://doi.org/10.1016/j.tree.2007.10.013>
- Robertson G (2000) GS+: Geostatistics for the environmental sciences. Gamma Design Software, Plainwell
- Rogers LJ, Moore LJ, Goldstein EB, Hein CJ, Lorenzo-Trueba J, Ashton AD (2015) Anthropogenic controls on overwash deposition: evidence and consequences. *Journal of Geophysical Research: Earth Surface* 120(12):2609–2624. <https://doi.org/10.1002/2015JF003634>
- Roman CT, Nordstrom KF (1988) The effect of erosion rate on vegetation patterns of an east coast barrier island. *Estuar Coast Shelf Sci* 26(3): 233–242. [https://doi.org/10.1016/0272-7714\(88\)90062-5](https://doi.org/10.1016/0272-7714(88)90062-5)
- Sallenger AH Jr, Doran KS, Howd PA (2012) Hotspot of accelerated sea-level rise on the Atlantic coast of North America. *Nat Clim Chang* 2(12):884–888. <https://doi.org/10.1038/nclimate1597>
- Scheffer M, Carpenter SR, Dakos V, van Nes EH (2015) Generic indicators of ecological resilience: inferring the chance of a critical transition. *Annu Rev Ecol Evol Syst* 46:145–167. <https://doi.org/10.1146/annurev-ecolsys-112414-054242>
- Schwarz C, Gourgue O, Van Belzen J, Gourgue O, van Belzen J, Zhu Z, Bouma TJ, van de Koppel J, Ruessink G, Claude N, Temmerman S (2018) Self-organization of a biogeomorphic landscape controlled

- by plant life-history traits. *Nat Geosci* 11(9):672–677. <https://doi.org/10.1038/s41561-018-0180-y>
- Seminack CT, McBride RA (2015) Geomorphic history and diagnostic features of former tidal inlets along Assateague Island, Maryland-Virginia: a life-cycle model for inlets along a wave dominated barrier islands. *Shore and Beach* 83(3):3–24
- Short AD, Hesp PA (1982) Wave, beach and dune interactions in south-eastern Australia. *Mar Geol* 48(3):259–284. [https://doi.org/10.1016/0025-3227\(82\)90100-1](https://doi.org/10.1016/0025-3227(82)90100-1)
- Stallins JA (2005) Stability domains in barrier island dune systems. *Ecol Complex* 2(4):410–430. <https://doi.org/10.1016/j.ecocom.2005.04.011>
- Stallins JA, Corenblit D (2018) Interdependence of geomorphic and ecological resilience properties in a geographic context. *Geomorphology* 305:76–93. <https://doi.org/10.1016/j.geomorph.2017.09.012>
- Stutz ML, Pilkey OH (2011) Open-ocean barrier islands: global influence of climatic, oceanographic, and depositional settings. *J Coast Res* 27(2):207–222. <https://doi.org/10.2112/09-1190.1>
- Thoms MC, Meitzen KM, Julian JP, Butler DR (2018) Biogeomorphology and resilience thinking: common ground and challenges. *Geomorphology* 305:1–7. <https://doi.org/10.1016/j.geomorph.2018.01.021>
- Weerman EJ, van de Koppel J, Eppinga MB, Montserrat F, Liu QX, Herman PMJ (2010) Spatial self-organization on intertidal mudflats through biophysical stress divergence. *Am Nat* 176(1):E15–E32. <https://doi.org/10.1086/652991>
- Williams A, Leatherman S (1993) Process form relationships of USA east coast barrier islands. *Z Geomorphol* 37(2):179–197
- Wohl E (2018) Geomorphic context in rivers. *Prog Phys Geogr* 42(6):841–857
- Wolner CW, Moore LJ, Young DR, Brantley ST, Bissett SN, McBride RA (2013) Ecomorphodynamic feedbacks and barrier island response to disturbance: insights from the Virginia barrier islands, mid-Atlantic bight, USA. *Geomorphology* 199:115–128. <https://doi.org/10.1016/j.geomorph.2013.03.035>
- Wu Q, Guo F, Li H, Kang J (2017) Measuring landscape pattern in three dimensional space. *Landsc Urban Plan* 167:49–59. <https://doi.org/10.1016/j.landurbplan.2017.05.022>
- Yousefi Lalimi F, Silvestri S, Moore L, Marani M (2017) Coupled topographic and vegetation patterns in coastal dunes: remote sensing observations and ecomorphodynamic implications. *Journal of Geophysical Research: Biogeosciences* 122(1):119–130. <https://doi.org/10.1002/2016JG003540>
- Zaremba RE, Leatherman SP (1986) Vegetative physiographic analysis of a US northern barrier system. *Environ Geol Water Sci* 8(4):193–207. <https://doi.org/10.1007/BF02524947>
- Zinnert JC, Shiflett SA, Via S, Bissett S, Dows B, Manley P, Young DR (2016) Spatial-temporal dynamics in barrier island upland vegetation: the overlooked coastal landscape. *Ecosystems* 19(4):685–697. <https://doi.org/10.1007/s10021-016-9961-6>
- Zinnert JC, Via SM, Nettleton BP, Tuley PA, Moore LJ, Stallins JA (2019) Connectivity in coastal systems: barrier island vegetation influences upland migration in a changing climate. *Glob Chang Biol* 25(7):2419–2430. <https://doi.org/10.1111/gcb.14635>

Publisher's note Springer Nature remains neutral with regard to jurisdictional claims in published maps and institutional affiliations.